Ecosystems (2026) 29:72
https://doi.org/10.1007/s10021-026-01099-3

© 2026 The Author(s)

ORIGINAL ARTICLE

Ditch Sediment Contribution to Remove Geogenic Nitrogen in a Reclaimed Area (Po River Delta, Italy)

Maria Pia Gervasio,[1] Fabio Vincenzi,[1] Nicolò Colombani,[2] Mattia Gaiolini,[3] Chiara Sbarbati,[3] Micol Mastrocicco,[4] Giuseppe Castaldelli,[1] and Elisa Soana[1]*

[1]*DiSAP - Department of Environmental and Prevention Sciences, University of Ferrara, Via Luigi Borsari, 46, 44121 Ferrara, Italy;* [2]*SIMAU – Department of Materials, Environmental Sciences and Urban Planning, Marche Polytechnic University, Via Brecce Bianche 12, 60131 Ancona, Italy;* [3]*DEB – Department of Ecological and Biological Sciences, University of Tuscia, Largo Università snc, 01100 Viterbo, Italy;* [4]*DiSTABiF – Department of Environmental, Biological and Pharmaceutical Sciences and Technologies, Campania University "Luigi Vanvitelli", Via Vivaldi 43, 81100 Caserta, Italy*

Abstract

Networks of drainage ditches play a crucial role in processing N loads along the land–river–sea system. This study investigated the N removal capacity of ditch sediments in a reclaimed area with paleo-marsh peat lenses releasing geogenic N to surface waters (Po River Delta, Italy). Sediment–water fluxes of O_2, inorganic N and N_2O, as well as denitrification and DNRA (dissimilatory nitrate reduction to ammonium) rates, were measured in spring and summer via incubations of intact sediment cores sampled at two sites having different pedological characteristics (silty clay loam and organic silty clay). The NO_3^- removal rate (247–534 μmol N m^{-2} h^{-1}) was primarily due to denitrification in both seasons, with a low amount recycled into NH_4^+ by DNRA (6–11%) and negligible conversion to N_2O (< 7‰). Under dark conditions, denitrification rates were higher in summer than in spring, driven by higher temperatures that stimulated microbial activity and oxygen consumption. Under light conditions, particularly in spring, coupled nitrification–denitrification was enhanced by microphytobenthos whose photosynthetic activity turned the sediment into a net oxygen source. Enrichment experiments suggested that denitrification was primarily controlled by NO_3^- availability whose production from nitrification can be limited in organic-rich sediments by oxygen shortage. Although the agricultural ditch system plays a significant role in dissipating N loads, removing NH_4^+ produced from the peat layers requires larger treatment areas or longer retention times, particularly in summer when the risk of eutrophication in coastal zones is greatest. Future

Received 31 March 2026; accepted 22 July 2026

Author Contributions Maria Pia Gervasio did investigation, formal analysis, visualization, writing—original draft; Fabio Vicenzi performed investigation, resources; Nicolò Colombani did investigation, formal analysis, writing—review and editing; Mattia Gaiolini did investigation, formal analysis; Chiara Sbarbati contributed in writing—review and editing; Micòl Mastrocicco helped in writing—review and editing; Giuseppe Castaldelli performed writing—review and editing, supervision; Elisa Soana did conceptualization, investigation, methodology, writing—review and editing, validation, funding acquisition, project administration, supervision.

*Corresponding author; e-mail: elisa.soana@unife.it

Published online: 13 August 2026

management and restoration strategies for lowland watersheds must take into account these internal geogenic sources, since they can circumvent standard nutrient reduction measures.

Key words: Denitrification; DNRA; Sediments; Agricultural ditches; Geogenic nitrogen; Eutrophication; Po River lowland.

Introduction

In Europe, the input of reactive nitrogen (N) has tripled throughout the twentieth century, primarily due to the use of inorganic fertilizers in agriculture to increase food production (de Vries and others, 2024). The N application often in excess of crop demand resulted in unintentional losses to both surface water and groundwater causing multiple detrimental consequences on chemical and biological quality, provision of ecosystem services, greenhouse gas emissions and human health (Battye and others, 2017; Adebanjo-Aina & Oludoye, 2025). After biodiversity loss and climate change, N-related environmental issues such as nitrate (NO_3^-) contamination and eutrophication are considered the third major global threat (Richardson and others, 2023). In Europe, more than half of surface water bodies are far from meeting the requirements for good ecological status (2000/60/EC), primarily due to high N concentrations (Nikolaidis and others, 2022) and the N accumulation in anthropogenic landscapes (that is, N legacy) can hinder the achievement of water quality goals in the short to medium term (Basu and others, 2022).

Many questions regarding the transformations and fate of N excess in human-impacted watersheds remain unanswered, and a significant proportion of the generated N load is retained internally rather than being delivered to terminal water bodies via river export (Schlesinger, 2009; Romero and others, 2021). The watershed high retention capacity can hide both permanent removal processes converting nitrate (NO_3^-) to dinitrogen gas (N_2) via biogeochemical reactions such as denitrification, anammox (anaerobic ammonium oxidation) and pyrite oxidation coupled with NO_3^- reduction, and temporary removal processes, such as storage in the vadose zone–groundwater system. It can also mask N loss to the atmosphere in the form of the greenhouse gas nitrous oxide (N_2O), as well as processes converting N from one reactive form to another, such as DNRA (dissimilatory nitrate reduction to ammonium) (Burgin & Hamilton, 2007; Balestrini and others, 2021; Basu and others, 2022).

Intensive agricultural practices, urbanization, and alterations to the river hydromorphology have contributed to the removal of natural filters (for example, wetlands, ponds, vegetated riparian zones), impairing the catchment buffering capacity and accelerating the nutrient transport from arable land to coastal areas (Racchetti and others, 2011; Bertassello and others, 2025). Artificial canal networks, which serve the purposes of irrigation, drainage and flood control, have become integral components of hydraulic-regulated agricultural settings, taking the place of natural riverine environments, progressively lost, in providing key ecological functions such as nutrient attenuation (Castaldelli and others, 2015; Veraart and others, 2017; Clifford and others, 2025). Due to their location at the interface between land and main water bodies, canals and ditches are important sites for N removal, thanks to the large nutrient inputs received, relative long retention times, capillary distribution and high biogeochemical transformation rates (Shen and others, 2021; Soana and others, 2023). This crucial ecosystem service is linked to microbial processes occurring in sediments among which heterotrophic denitrification generally dominates, that is, anaerobic respiration where NO_3^- acts as terminal electron acceptor for organic matter oxidation and is reduced into N_2, through several intermediates, including N_2O. The three primary drivers that directly affect the magnitude of denitrification (anoxic conditions, the availability of NO_3^- and organic carbon) are found in ditch sediments (Veraart and others, 2017; Soana and others, 2023). During the irrigation period, large volumes of water are withdrawn from water bodies and redistributed across the landscape via networks of canals and ditches. This provides more opportunity for N transformation and loss due to the increased flow path lengths and the high temperatures that stimulate microbial processes (Smith and others, 2006; Romero and others, 2021; Speir and others, 2023). Under strongly reducing conditions typical of organic-rich sediment in summer, NO_3^- can also be converted to ammonium (NH_4^+) by DNRA, but in contrast to denitrification, the recycled N remains within the system (Burgin & Hamilton, 2007; Scott and others, 2008; Speir and others, 2023).

Ditches and canals are the first point of contact for diffuse and point N loads entering the hydrological network, but they can also become polluted by NO_3^--rich seeping up from aquifers where

NO_3^- from agriculture has accumulated (Balestrini and others, 2021). In addition to being sources of anthropogenic NO_3^- to surface waters, aquifers and often aquitards act also as suppliers of naturally occurring geogenic NH_4^+, associated with the long-term decomposition of sedimentary organic matter (SOM), typical of many deltaic and lowland areas around the world (Mastrocicco and others, 2013; Xiong and others, 2025; Liu and others, 2026). The attenuation of NH_4^+ in surface water via coupled nitrification–denitrification has received comparatively little attention, despite groundwater–surface water interaction and intensive aquifer exploitation to meet irrigation demands contribute to water quality deterioration and eutrophication of vulnerable coastal zones (Sawyer and others, 2016; Lewandowski and others, 2020). Research efforts should investigate the mechanisms governing N cycling and fate along the terrestrial–freshwater–coastal continuum in agricultural watersheds to identify those processes that remove it completely. This would drive the adoption of strategy to decrease the eutrophication potential of the water volumes conveyed to the coastal zone, while at the same time minimizing the greenhouse gas emissions.

The present study aims to evaluate the importance of sediment-driven NO_3^- removal pathways (denitrification and DNRA) by conducting in situ incubations of intact sediment cores sampled from ditches impacted by geogenic N loads from SOM-rich deposits (Po River Delta, Italy). Spring and summer were selected as the seasons posing the greatest risk of eutrophication in coastal zones, due to the combination of high temperatures and N from agricultural runoff triggering algal blooms (Romero and others, 2013; Gervasio and others, 2024a). It is exactly during these seasons that the crucial role of canal networks as buffering systems is most important.

Material and Methods

Study Area

The experimental site is located in the Po River lowland near the village of Berra (44° 56′ 54.87′′ N, 12° 01′ 26.66′′ E, −3 a.s.l., Emilia-Romagna Region, Italy), approximately 24 km from the Adriatic Sea. The area belongs to the Po di Volano-Sacca di Goro watershed (Figure 1a), the terminal portion of the Po River Basin, a reclaimed deltaic territory included within the administrative borders of the Ferrara Province. The Po di Volano is an ancient branch of the Po River Delta, which has been converted into an artificial canal carrying water to the Sacca di Goro lagoon. The climate is sub-humid, and most of the watershed lies below sea level in a depressed area. Thus, the hydrological regime is artificially regulated by a network of canals, pumping stations and gates, which are managed by the Ferrara Land Reclamation Consortium. The large availability of freshwater resources for irrigation and the flat morphology of the territory favored the development of intensive agricultural activity, which is almost entirely dependent on synthetic fertilizers.

The experimental site is located in a highly anthropized agricultural landscape, characterized by an annual crop rotation of wheat and maize (Figure 1b). In 2024, when the study was carried out, the field plot was cultivated with maize and subirrigated with tile drains to minimize evaporation. The subsurface drainage system consists of a series of 9 cm diameter perforated PVC pipes spaced 10 m apart. It helps to drain excess water from the shallow unconfined aquifer, thereby preventing waterlogging and guaranteeing an oxic/suboxic environment, where NO_3^- is the dominant N species (Macumu and others, 2024; Gaiolini and others, 2026). Earthen drainage ditches collect water from the tile drains and finally deliver it to the main collector. Sediment cores were collected from two shallow ditches (water depth < 15 cm), that is, P bordering the field plot cultivated with maize, and PP bordering an uncultivated plot characterized by near-surface peaty horizons (Figure 1b). Scattered patches of helophytic vegetation (*Phragmites australis*) grow along the banks of both ditches, but the sediment is completely unvegetated. During the non-irrigation period, the average flow rate is less than 0.5 L s^{-1}, whereas during the irrigation period, the ditches also drain excess irrigation water withdrawn from the Albersano irrigation canal (located upstream of the P site), with the flow rate averaging at around 4 L s^{-1}. The two ditches have different pedological characteristics, that is, silty clay loam for P and organic silty clay for PP, the two most common sediment types in the investigated basin (Gaiolini and others, 2026). Peaty lenses, formed from fragments of marsh lagoonal vegetation, are characteristic of the complex stratigraphic evolution of the study basin. Peaty and organic clay layers are preserved in the shallow sediments of around 20% of the Po di Volano basin area (Bruno and others, 2022), acting as a long-term source of geogenic N for surface watercourses that receive drained water from waterlogged peaty lenses. The presence of peaty horizons, in combination with the low hydraulic

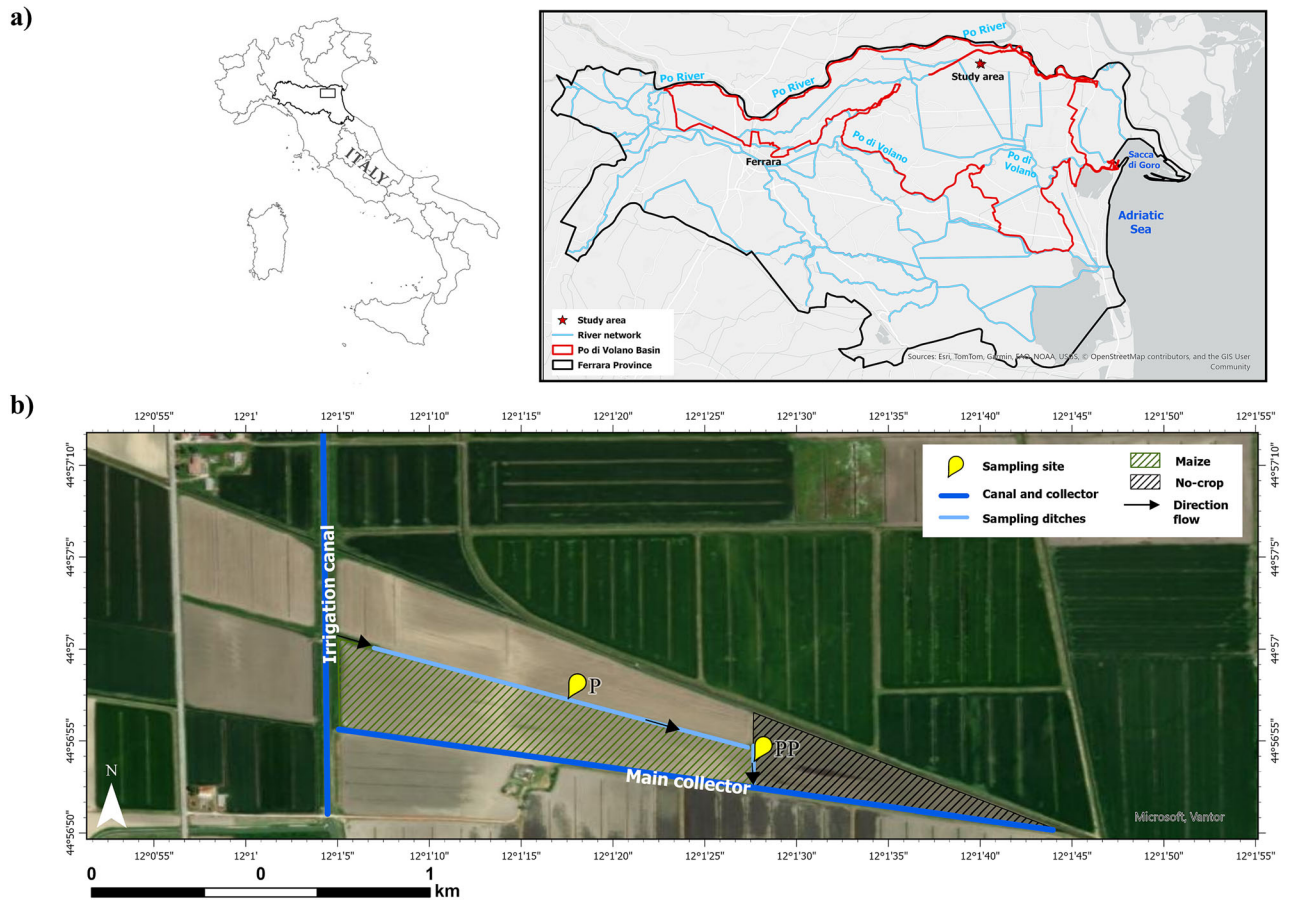


Figure 1. Map of the study site. **a** Location of the study area (red star) within the Po di Volano basin (red area); **b** location of the sampling ditches (P and PP) within the agricultural plot. The basemap is modified in ArcGISPro 2025 (ESRI, Redlands, California).

conductivity of the sediments, triggers the SOM degradation and the mineralization of organic N into NH_4^+, which feeds surface waters, as demonstrated via stable isotopes at several sites in the Po River lowland (Mastrocicco and others, 2013; Colombani and others, 2019).

Sediment Sampling and Incubation Activities

Sampling campaigns were conducted in spring (May 2024) and summer (July 2024), the latter overlapping with an irrigation event. The experimental design consisted of thirteen intact sediment cores (Plexiglass liners, internal diameter 4.5 cm, length 20 cm) collected by hand from each ditch in spring and summer. The cores were checked and levelled to achieve a sediment height of around 9 cm and an overlying water column of around 8 cm. During each sampling, 50 L of ditch water for the pre-incubation and incubation phases was collected downstream of the PP site, just before entering the main collector. Water temperature was measured in situ using a multiparametric probe (YSI, Model 85, Yellow Springs, OH, USA).

Sampling, pre-incubation, and incubation procedure were performed according to standardized protocols (Dalsgaard and others, 2000; Owens and Cornwell, 2016). Ten cores for each site per season were incubated for benthic flux and denitrification measurements, while the remaining three cores for each site were used for the sediment characterization. Dark and light incubations were performed to detect the effect of photosynthetic activity on benthic N processing. Five sediment cores per site were randomly assigned to each treatment, transferred into separate tanks corresponding to light and dark conditions, and submerged by unfiltered ditch water. The tanks were placed in an unshaded area near the sampling sites, and incubations were performed in situ. The sediment cores were kept continuously aerated using aquarium pumps overnight until the start of the incubations. The

liners were left open at the top to allow the exchange of water within the cores with aerated and mixed water in the tank.

Each core was equipped with a rotating Teflon-coated magnetic bar suspended in the water column a few centimeters above the sediment surface and connected to an external unit rotating at 40 rpm, avoiding the sediment resuspension. In line with seasonal averages for slow-flowing shallow waterways in the study area (Soana and others, 2023), the cores were kept at the daily average field temperature, that is, ~ 19 °C and ~ 27 °C in spring and summer, respectively. The temperature in the incubation tanks was controlled using a thermostat and monitored continuously using a multi-parameter probe. The day after sampling, the water in the tanks was replaced with fresh water from the sampling site to maintain nutrient concentrations found in the field (NO_3^-: 140 µM in spring and 100 µM in summer; NH_4^+: 90 µM in spring and 20 µM in summer). To start the benthic flux incubation, the water level in the tanks was lower to isolate the cores (~ 2 cm from the upper edge of the liners), and each one was closed with opaque or transparent floating lids. Dark and light incubations were conducted simultaneously between 11 a.m. and 4 p.m., when irradiance levels were at their highest during the day. The average irradiance during incubations was ~ 440 W m^{-2} and ~ 590 W m^{-2} in spring and summer, respectively (data from ''Malborghetto'' station, available online from Regional Agency for Environmental Protection and Prevention of the Emilia-Romagna Region—ARPAE, https://simc.arpae.it/dext3r/). For the dark treatment, the cores were wrapped in aluminum foil, and the tank was enclosed in a black bag to prevent light exposure. Incubation times ranged from 2 (summer experiment) to 4 (spring experiment) hours and were set, based on pilot tests, as the minimum time needed to detect significant changes in solute concentration while maintaining oxygen concentrations at the end of the incubation within ±20–30% of the initial value (Owens and Cornwell, 2016). At the beginning and the end of the incubation, dissolved oxygen concentrations (O_2; µM) were measured with a multiparametric probe, and water samples were collected from each core using a glass 60 mL syringe. Samples for N_2O determination were transferred to 20 mL glass vial through a gas-tight tubing until overflow, fixed with 7 M $ZnCl_2$ to stop the microbial activity and sealed with a butyl rubber septum without headspace for gas chromatography analysis. The remaining water sample was filtered with glass fiber filters (Whatman GF/F, 0.7 µm pore size), transferred to 20 mL polyethylene scintillation vials, and stored at − 20 °C for the spectrophotometric analyses of the dissolved inorganic N concentrations (NO_3^-, NO_2^-, and NH_4^+).

After the benthic flux incubation, the cores were submerged and left uncapped until the subsequent incubation. In the second incubation, the Isotope Pairing Technique (IPT; Nielsen, 1992) was applied to measure the denitrification and DNRA rates. Due to the longer incubation times in spring, the IPT experiment was carried out the following day, ensuring the cores remained aerated overnight as in the pre-incubation phase. By contrast, in summer, the two incubations took place consecutively to avoid the impact of high temperatures on microbial processes causing the sedimentary N pool to deviate from the initial conditions. Sequential incubations minimized the effects of core aging, enabling reliable comparisons to be made between benthic fluxes and denitrification rates. In between incubations (~ 1 h), the cores were maintained with the top uncapped and submersed in renewed ditch water to restore chemical gradients. Similar to the benthic flux incubation, the water level in the tank was lowered to isolate the cores and initiate the experiment, after water temperature and electrical conductivity (EC; µS cm^{-1}) were measured. An aliquot (according to the water volume in each column) of a stock solution of 20 mM $^{15}NO_3^-$ ($Na^{15}NO_3$, Sigma Aldrich, ≥ 98 atom% enrichment) was added to each core to obtain a final $^{15}NO_3^-$ enrichment of 40–90%. Water samples were collected in each core before and after the addition of $^{15}NO_3^-$ to calculate the ^{14}N:^{15}N ratio in the NO_3^- pool. After the addition, the cores were pre-incubated without lids for 15 min to allow the labeled tracer to diffuse into the sediment NO_3^- reduction zone (Nielsen, 1992). The cores were then sealed with opaque or transparent lids for the dark and light treatments, respectively, and left to incubate within the timeframe and manner described above. At the end of the incubation, dissolved N_2 pools in the water column and porewater were homogenized by gently stirring the sediment with a plastic bar. Slurries were briefly allowed to settle and collected by a glass 60 mL syringe with attached tubing. Subsamples were transferred to 12 mL glass-tight vials (Exetainer®, Labco Limited, Lampeter, UK) and fixed with 200 µL of 7 M $ZnCl_2$ to stop microbial activity. The vials were kept refrigerated with the upside-down orientation for subsequent analysis of the $^{28}N_2$; $^{29}N_2$ and $^{30}N_2$ composition of the dissolved N_2 pool.

A 50 mL aliquot of slurry was sampled from each core to determine DNRA rates from the production

of $^{15}NH_4^+$, as previously reported by Gervasio and others (2024a). Briefly, samples were treated with KCl (2 M), shaken for 30 min and centrifugated (1800 rpm for 15 min). The supernatant was filtered through Whatman GF/F glass fiber filters and transferred to 20 mL polyethylene scintillation vials. The vials were air-purged for 10 min to eliminate $^{29}N_2$ and $^{30}N_2$ pools generated during the IPT incubation, transferred into 12 mL glass-tight vial (Exetainer®, Labco Limited, Lampeter, UK), and treated with 200 µL of alkaline hypobromite solution to oxidize all the NH_4^+ to N_2 (Warembourg, 1993). Samples were then refrigerated until they were analyzed for $^{28}N_2$, $^{29}N_2$ and $^{30}N_2$.

Analytical Methods and Calculation of Benthic Fluxes and N Process Rates

Nitrate was determined by using the cadmium reduction method on a Technicon Autoanalyzer (Armstrong and others, 1967). Ammonium and nitrite were analyzed via standard colorimetric methods using a UV/Vis spectrophotometer (V-550, Jasco International, Tokyo, Japan). Ammonium was measured using salicylate and hypochlorite in the presence of sodium nitroprusside (Bower and Holm-Hansen, 1980). Nitrite was measured using sulfanilamide and N-(1-naphthyl)-ethylenediamine (APHA, 1992). The $^{28}N_2$:Ar, $^{29}N_2$:$^{28}N_2$ and $^{30}N_2$:$^{28}N_2$ ratios in samples from IPT incubations were analyzed using membrane inlet mass spectrometry (MIMS, Bay Instruments, Easton MD, USA) (Kana and others, 1994; Boedecker and others, 2024). Dissolved $^{28}N_2$ concentration was calculated by multiplying the observed $^{28}N_2$:Ar ratio by the theoretical Ar saturation value derived from the gas solubility tables based on the sampling temperature and EC (Weiss, 1970). Gas samples for dissolved N_2O measurement were extracted from water according to the headspace equilibration method (de la Paz and others, 2021; Weiss and Price, 1980) and analyzed by a Trace 1600 gas chromatograph (Thermo Fisher Scientific Inc.) equipped with an Electron Capture Detector and a TriPlus robotic autosampler.

Hourly dark and light benthic fluxes of dissolved gases (O_2, N_2O) and nutrients (NO_3^-, NO_2^-, NH_4^+) were calculated from the difference between final and initial concentration in the water column, according to following equation (Owens and Cornwell, 2016):

$$F_x = \frac{(C_f - C_0) \cdot V}{A \cdot t} \quad (1)$$

where F_x is the flux of x-solute or x-gas (µmol m^{-2} h^{-1}), C_f and C_0 are final and initial concentrations of x (µM), respectively; V (L) is the water volume inside the core, A is the sediment surface area inside the core (m^2), and t is the time of incubation (h). Positive and negative fluxes indicate an increase or decrease in the concentration of a solute in the water phase, respectively. Positive fluxes indicate net solute production, that is, the release of solutes from the sediment to the water column. Negative fluxes, on the other hand, indicate net consumption, that is, the removal of solutes from the water column. Nitrite exchanges across the water–sediment interface resulted negligible compared to NO_3^- fluxes; therefore, data were not shown.

Denitrification rates (µmol N m^{-2} h^{-1}) were obtained according to the principles and equations proposed by Nielsen (1992) and reviewed by Steingruber and others (2001), based on a binomial distribution of $^{28}N_2$, $^{29}N_2$ and $^{30}N_2$:

$$D_{15} = p29 + 2p30 \quad (2)$$

$$D_{14} = D_{15} \cdot \left(\frac{p29}{2p30}\right) \quad (3)$$

$$D_{tot} = D_{14} + D_{15} \quad (4)$$

where D_{15} is the denitrification rate of the added $^{15}NO_3^-$, p29 and p30 are the production rates of $^{29}N_2$ and $^{30}N_2$, respectively, D_{14} is the denitrification rate of $^{14}NO_3^-$, D_{tot} is the total denitrification rate.

Denitrification of the $^{14}NO_3^-$/$^{15}NO_3^-$ mixture diffusing from the water column into the sediment ($D_w$tot) was calculated, according to Steingruber and others (2001):

$$D_w^{tot} = \frac{D_{15}}{\varepsilon} \quad (5)$$

where ϵ is the isotopic NO_3^- enrichment in the IPT incubation, obtained as:

$$\varepsilon = \frac{C_a - C_b}{C_a} \quad (6)$$

where C_a and C_b are NO_3^- concentrations (µM) after and before the $^{15}NO_3^-$ tracer addition, respectively.

Coupled nitrification–denitrification (D_n), that is, denitrification of NO_3^- produced in the oxygen sediment layer by nitrification was obtained by difference as:

$$D_n = D_{tot} - D_w^{tot} \quad (7)$$

Assuming a linear relationship between $^{15}NO_3^-$ concentrations and the overall denitrification rate D_w^{tot}, the effective rate can be extrapolated back to tracer-free conditions. This enabled the quantification of the denitrification rate D_w associated with the ambient nitrate ($^{14}NO_3^-$) diffusing from the water column to the sediment:

$$D_w = D_w^{tot} \cdot (1 - \varepsilon) \quad (8)$$

The presence of anammox disrupts the application of IPT, resulting in an overestimation of the rates, since the N_2 produced by anammox cannot be differentiated from that produced by denitrification (Risgaard-Petersen and others, 2003). The coexistence of anammox and denitrification contradicts the assumption that the production of $^{28}N_2$ is independent of the concentration of added $^{15}NO_3^-$. Indeed, anammox combines added $^{15}NO_3^-$ with unlabeled $^{14}NH_4^+$ in sediments to produce additional $^{29}N_2$, making the binomial distribution of ^{14}N and ^{15}N in the N_2 pools not fulfilled (Robertson and others, 2019). The contribution of anammox to total N_2 production in sediments was as evaluated by preliminary anoxic slurry incubations (Risgaard-Petersen and others, 2003) and was found to be $< 0.03\%$. Furthermore, the $^{28}N_2$ production measured during the IPT incubations of intact sediment cores showed no correlation with added $^{15}NO_3^-$ concentrations. This excluded the possibility of a significant overestimation of denitrification rates due to anammox, thus validating the application of the IPT technique and the equations proposed by Nielsen (1992).

Similar to denitrification, the total DNRA rates were calculated according to Risgaard-Petersen and Rysgaard (1995) and under the assumption that the two processes occurred within the same sediment horizon. The total DNRA rates were divided into DNRA of water column NO_3^- ($DNRA_w$) and DNRA coupled to nitrification ($DNRA_n$).

Sediment Characterization

Three cores for site were processed as follows for sediment characterization. They were extruded, and the upper 0–1 cm sediment depth horizon was rapidly homogenized to determine sediment features. Aliquots of 5 mL were collected using a cutoff syringe and weighed to determine density, which is defined as the ratio of wet weight to volume. Porosity was determined by measuring the weight loss of a known volume of fresh sediment after drying at 50 °C for 48 h. Powdered dried samples were placed in a muffle furnace at 350 °C for three hours to quantify the organic matter content (OM, %), based on weight loss by ignition (LOI). Benthic microalgal biomass was measured as sedimentary chlorophyll-a (Chl-a) concentration. The pigment was extracted from the sediment (2 mL) with acetone (90%), in the dark at 4 °C for 24 h, centrifugated and subsequently determined spectrophotometrically (Lorenzen, 1967).

Statistical Analysis

All statistical analysis was performed using a generalized linear model (GLM) with the RStudio software (version 2023.06.0–421). The standard linear model (LM) was applied to analyze water–sediment fluxes of O_2, N_2O, NO_3^- and NH_4^+, denitrification (D_w, D_n and D_{tot}) and DNRA ($DNRA_w$, $DNRA_n$ and $DNRA_{tot}$) rates and their third-order interactions. The LM was performed via the *lme4* RStudio-package (Bates and others, 2015). The fixed factors were the sites (P and PP), the seasons (spring and summer) and the illumination conditions (light and dark) and their interactions. The sample size was equal for all tests, and core was included as a random effect in LM. The statistical significance of the primary effects and interaction terms was evaluated by means of Analysis of Variance (ANOVA) Type III, performed via *car* RStudio-package (Fox and Weisberg, 2019). ANOVA Type III was employed to assess the unique contribution of each factor to the model as a whole. Linear regression was applied to detect the dependency of $D_w$tot from NO_3^- availability ($^{14}NO_3^-$ + $^{15}NO_3^-$) in water column. Statistical significance was set at a p level ≤ 0.05.

Results and Discussion

Benthic Metabolism and Dissolved Inorganic N Fluxes in Ditch Sediments

Benthic O_2 fluxes were strongly influenced by season and illumination conditions, as well as the interaction between the two ($p < 0.001$; Table 1). At P site, dark O_2 fluxes were always negative, ranging from -2167 ± 413 (spring, Figure 2a) to -3539 ± 357 µmol O_2 m^{-2} h^{-1} (summer, Figure 2b), indicating consumption thought respiration processes and SOM mineralization. As PP site, O_2 fluxes ranged from -1062 ± 171 (spring) to -2772 ± 125 µmol O_2 m^{-2} h^{-1} (summer). Dark O_2 consumption rates measured at both sites, overlapping the typical values reported in the literature for freshwater eutrophic environments (Scott and others, 2008; Racchetti and others, 2011; Castaldelli and others, 2015), were found to be higher

Table 1. Effects of Factor Season (Spring and Summer), Site (P and PP) and Illumination Condition (Light and Dark) on Benthic Fluxes and N Process Rates, Analyzed Using Generalized Linear Model (GLM) with ANOVA (Type III)

Parameters	Factor	d*F*	*F*	*p*
O_2 flux	Site	1	5.8	< **0.05**
	Illumination	1	51.8	< **0.001**
	Season	1	8.9	< **0.01**
	Site x Illumination	1	0.1	0.74
	Site x Season	1	0.3	0.61
	Illumination x Season	1	15.7	< **0.001**
	Site x Illumination x Season	1	0.5	0.47
NO_3^- flux	Site	1	0.5	0.48
	Illumination	1	11.3	< **0.01**
	Season	1	1.8	0.20
	Site x Illumination	1	3.2	0.08
	Site x Season	1	0.3	0.57
	Illumination x Season	1	5.0	< **0.05**
	Site x Illumination x Season	1	1.6	0.22
NH_4^+ flux	Site	1	15.8	< **0.001**
	Illumination	1	41.6	< **0.0001**
	Season	1	0.01	0.91
	Site x Illumination	1	0.1	0.77
	Site x Season	1	1.0	0.31
	Illumination x Season	1	28.0	< **0.0001**
	Site x Illumination x Season	1	0.003	0.96
N_2O flux	Site	1	4.42	< **0.05**
	Illumination	1	0.22	0.64
	Season	1	2.26	0.14
	Site x Illumination	1	4.70	< **0.05**
	Site x Season	1	3.97	0.06
	Illumination x Season	1	1.48	0.23
	Site x Illumination x Season	1	1.43	0.24
Total denitrification rate	Site	1	0.05	0.82
	Illumination	1	11.1	< **0.01**
	Season	1	2.9	0.10
	Site x Illumination	1	0.0	0.98
	Site x Season	1	0.8	0.37
	Illumination x Season	1	4.7	0.05
	Site x Illumination x Season	1	0.01	0.90
Dw rate	Site	1	0.6	0.45
	Illumination	1	2.4	0.13
	Season	1	3.1	0.08
	Site x Illumination	1	0.4	0.54
	Site x Season	1	1.9	0.18
	Illumination x Season	1	1.5	0.23
	Site x Illumination x Season	1	0.4	0.54
Dn rate	Site	1	2.9	0.10
	Illumination	1	42.4	< **0.0001**
	Season	1	0.01	0.93
	Site x Illumination	1	4.4	< **0.05**
	Site x Season	1	1.4	0.25
	Illumination x Season	1	12.5	< **0.01**
	Site x Illumination x Season	1	2.2	0.15

Table 1. continued

Parameters	Factor	d*F*	*F*	*p*
Total DNRA rate	Site	1	0.02	0.91
	Illumination	1	0.0	0.97
	Season	1	1.7	< **0.01**
	Site x Illumination	1	0.02	0.88
	Site x Season	1	3.2	0.08
	Illumination x Season	1	0.2	0.64
	Site x Illumination x Season	1	1.4	0.24
DNRAw rate	Site	1	0.6	0.44
	Illumination	1	0.2	0.65
	Season	1	17.7	< **0.001**
	Site x Illumination	1	2.8	0.10
	Site x Season	1	4.1	< **0.05**
	Illumination x Season	1	1.1	0.30
	Site x Illumination x Season	1	1.5	0.23
DNRAn rate	Site	1	2.0	0.16
	Illumination	1	0.7	0.41
	Season	1	0.2	0.69
	Site x Illumination	1	1.4	0.24
	Site x Season	1	0.9	0.33
	Illumination x Season	1	3.4	0.07
	Site x Illumination x Season	1	0.4	0.55

The model includes all main effects and three-way interaction. Degrees of freedom (dF), F test value (F), and significance level (p) are reported. Significant differences ($p < 0.05$) are in bold

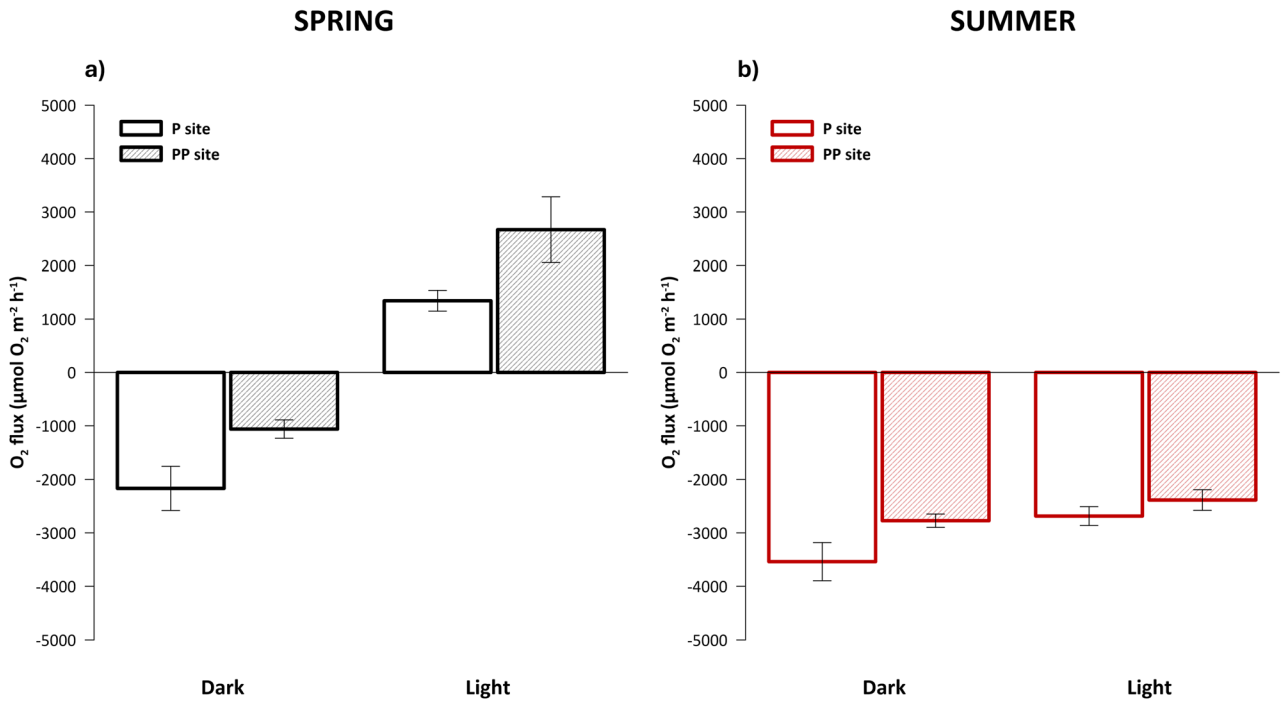


Figure 2. Benthic oxygen fluxes (µmol O_2 m^{-2} h^{-1}) measured at the two sites (P and PP), in dark and light conditions during **a** spring and **b** summer. Average values ± standard deviation are reported (n = 5).

Table 2. Density, Porosity, Organic Matter Content (%) and Chlorophyll-a Concentrations of Sediments at Sampling Sites

	Spring		Summer	
	P	PP	P	PP
Typology	silty clay loam	organic silty clay	silty clay loam	organic silty clay
Density ($g\ mL^{-1}$)	1.2 (0.1)	1.2 (0.1)	1.2 (0.6)	1.3 (0.7)
Porosity	0.8 (0.03)	0.7 (0.04)	0.6 (0.3)	0.6 (0.3)
SOM (%)	6 (0.5)	13 (0.4)	4 (1.0)	8 (1.0)
Chl-a ($mg\ m^{-2}$)	58.8 (8.4)	51.5 (18.3)	25.2 (7.0)	50.0 (5.6)

Standard Deviations are Reported in Brackets.

in summer than in spring, as temperature warming stimulated sediment respiration and decomposition rates (de Klein and others, 2017; Gervasio and others, 2024a). SOM was a poor predictor of dark O_2 demand, suggesting that organic matter lability rather than its quantity was the main driver of benthic respiration. Indeed, SOM content was higher at the PP site (Table 2) but consisted mainly of tissue fragments of halophilic vegetation hosted in peat layers (Macumu and others, 2024). This recalcitrant litter is resistant to degradation and results in low O_2 consumption. Light O_2 fluxes resulted positive in spring at both sites, ranging from 1342 ± 194 to 2669 ± 616 μmol O_2 m^{-2} h^{-1} at P and PP site, respectively, highlighting how the balance between O_2 production via photosynthesis and O_2 consumption via SOM mineralization was in favor of the former. The presence of microphytobenthos, as confirmed by sedimentary chl-a (Table 2), was responsible for the benthic O_2 production through photosynthetic activity in the light (Sundbäck and others, 1991; Zilius and others, 2012). Light O_2 fluxes resulted negative in summer at both sites, averaging at − 2685 ± 177 and − 2385 ± 193 μmol O_2 m^{-2} h^{-1}, at P and PP site, respectively (Figure 2b). Despite the presence of microphytobenthos, the sediments shifted toward net heterotrophy during the summer, likely to due to O_2 consumption resulting from mineralization processes driven by high temperatures, which exceeded O_2 production.

Benthic NO_3^- fluxes were always directed toward the sediment and significantly influenced by interaction between illumination condition and season ($p < 0.05$; Table 1). Both sites exhibited comparable seasonal variations in dark NO_3^- fluxes. Rates intensified from spring to summer, ranging from − 298 ± 43 μmol N m^{-2} h^{-1} to − 391 ± 71 μmol N m^{-2} h^{-1} at P site, and from − 247 ± 34 μmol N m^{-2} h^{-1} to − 399 ± 30 μmol N m^{-2} h^{-1} at PP site (Figure 3a, b). Despite lower NO_3^- availability (140 μM in spring and 100 μM in summer), the higher consumption rates in summer suggested that NO_3^- demand was more affected by temperature than by substrate availability (Gervasio and others, 2024a). In spring, light exposure significantly increased sediment NO_3^- demand at P site (up to − 534 ± 77 μmol N m^{-2} h^{-1}), promoting its removal through a combination of microphytobenthos assimilation and microbial dissimilative reduction (Sundbäck and others, 1991; Racchetti and others, 2017). Exchanges of NH_4^+ across the water–sediment interface were strongly influenced by sediment type ($p < 0.001$; Table 1). Higher effluxes were observed at PP than at P, likely due to the mineralization of N-rich peaty lenses (Mastrocicco and others, 2013; Gaiolini and others, 2026), which is consistent with porewater conditions found to be richer in NH_4^+ at PP (up to ∼ 1000 μM) than at P (∼ 200 μM) (data not shown). The only exception was in the spring, under light conditions, when both sites were found to be NH_4^+ sinks (Figure 3c, d). Statistical analyses revealed a significant interaction between illumination condition and season ($p < 0.0001$; Table 1). Dark benthic NH_4^+ fluxes were always positive, suggesting that variable fractions of ammonified N were neither retained within the sediments nor completely oxidized to NO_3^-. There was no substantial increase in the dark release of NH_4^+ with rising water temperatures from spring (∼ 19 °C) to summer (∼ 27 °C) (Figure 3c, d). The SOM content decreased from spring to summer (Table 2); therefore, the expected stimulating effect of higher

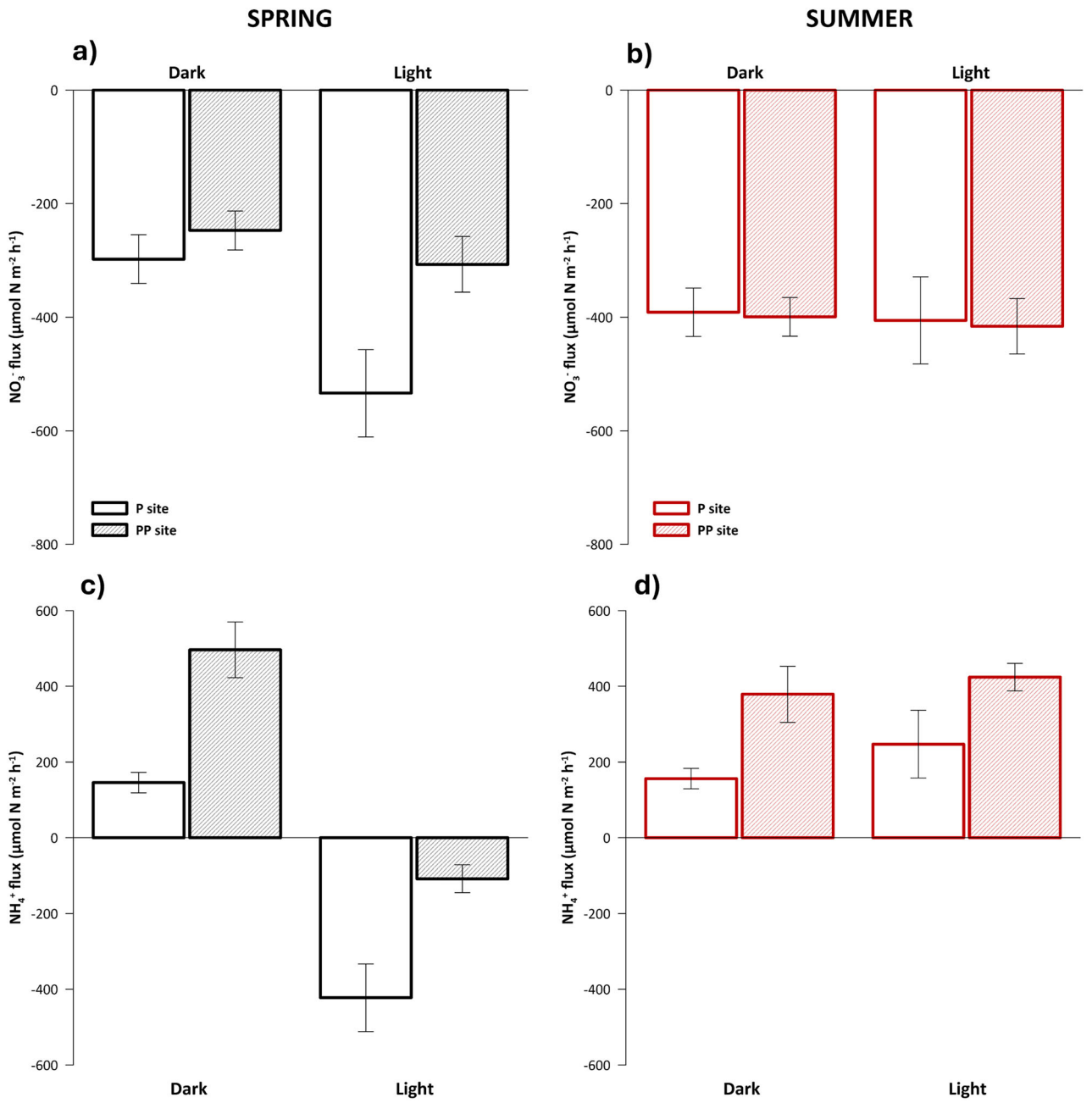


Figure 3. Benthic fluxes of NO_3^- (µmol N m^{-2} h^{-1}; on the top) and NH_4^+ (µmol N m^{-2} h^{-1}; on the bottom) measured at the two sites (P and PP), in dark and light conditions during **a–c** spring and **b–d** summer. Average values ± standard deviations are reported (n = 5); (note the different scale on the y-axis).

summer temperatures was likely counterbalanced by lower organic matter availability. In light conditions, NH_4^+ fluxes shifted from negative to positive in the spring–summer transition. Summer sediments released NH_4^+, while in spring, NH_4^+ uptake was measured, with higher values (− 422 ± 89 µmol N m^{-2} h^{-1}) at P site compared to PP site (− 108 ± 36 µmol N m^{-2} h^{-1}). Light conditions may promote the removal of NH_4^+ through microphytobenthos assimilation and nitrification (Zilius and others, 2012; Racchetti and others, 2017).

N Dynamics in Ditch Sediments

Total denitrification rates were significantly affected by the illumination conditions ($p < 0.01$; Table 1). D_{tot} was slightly higher in light compared to dark conditions (Figure 4a, b), ranging from

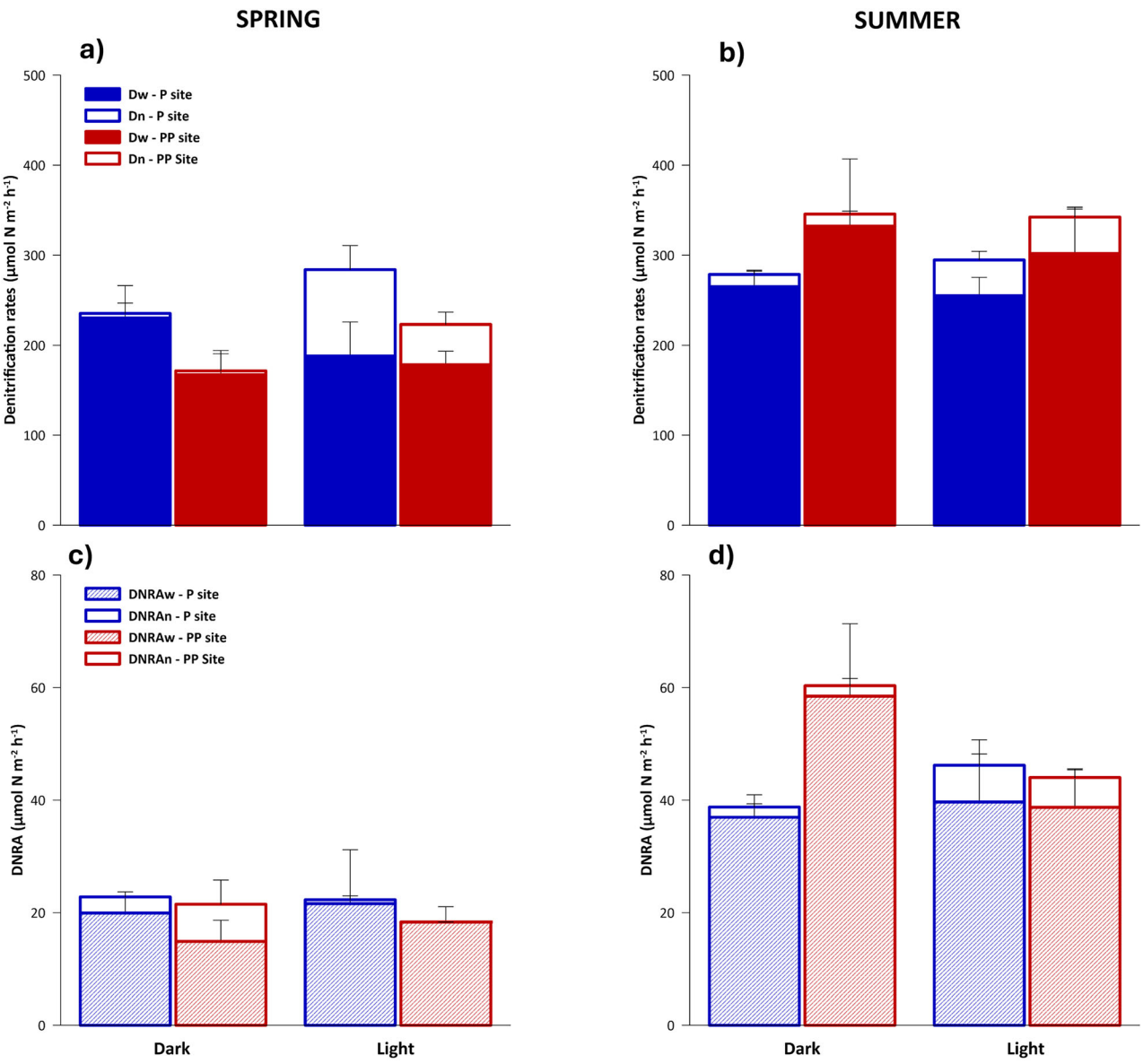


Figure 4. Total denitrification rates (µmol N m^{-2} h^{-1}; on the top) splitted into D_w and D_n measured at the two sites (P and PP), in dark and light conditions during **a** spring and **b** summer. Total dissimilative nitrate reduction to ammonium (DNRA) rates (µmol N m^{-2} h^{-1}; on the bottom) splitted into $DNRA_w$ and $DNRA_n$ measured in **c** spring and **d** summer in both sites (P and PP) in dark and light conditions. Average values ± standard deviations are reported (n = 5).

284 ± 65 µmol N m^{-2} h^{-1} (spring) to 295 ± 25 µmol N m^{-2} h^{-1} (summer) at P site and from 223 ± 37 µmol N m^{-2} h^{-1} (spring) to 342 ± 45 µmol N m^{-2} h^{-1} (summer) at PP site. These rates are consistent with those previously reported for eutrophic freshwater ecosystems in the Po River Basin (for example, Racchetti and others, 2011; Gervasio and others, 2022; Soana and others, 2023), as well as with rates observed worldwide (Pina-Ochoa & Álvarez-Cobelas, 2006). Total denitrification was mostly supported by water column NO_3^- (D_w), but the contribution of D_n was higher in light than in dark, accounting for 20–34% in spring and 12–14% in summer of the total rates. The availability of NO_3^- in the water column and the O_2 concentration in the benthic zone regulate the partitioning of total rates into D_w and D_n. As widely reported in the literature, D_w is usually dominant when water NO_3^- concentrations exceed 50 µM (Pina-Ochoa & Álvarez-Cobelas, 2006; Racchetti and others, 2011; Gervasio and others, 2024a). In dark conditions, total denitrification rates ranged from 235 ± 25 µmol N m^{-2} h^{-1} (spring) to 278 ± 19 µmol N m^{-2} h^{-1} (summer) at

P site and from 172 ± 11 μmol N m^{-2} h^{-1} (spring) to 343 ± 71 μmol N m^{-2} h^{-1} (summer) at PP site, with D_w accounting for 96–98% of the total rates.

The coupled nitrification–denitrification process was promoted by light conditions, especially in spring. Nitrification was stimulated by oxic conditions in the surface sediment triggered by the photosynthetic activity of microalgae, as evidenced by NH_4^+ being consumed from the water column (Figure 3c) in parallel with O_2 being produced (Figure 2a). The ammonified NH_4^+ was oxidized within the oxic sediment layer, generating NO_3^- that diffused into the deeper anoxic layer, where it was reduced to N_2, leading to D_n peaks (An & Joye, 2001; Racchetti and others, 2017). In summer, nitrification was only a minor source of NO_3^- for denitrification, limiting the complete dissipation of geogenic N loads. Increasing temperatures may trigger the enzyme kinetics of nitrifying bacteria, which are no longer limited by NH_4^+ derived from the mineralization of organic N stimulated by warmer conditions. However, higher water temperatures both reduce O_2 solubility and increase sedimentary O_2 consumption, limiting O_2 penetration and reducing the extension of oxic layer suitable for nitrifying bacteria (Rysgaard and others, 1994; Sundbäck and others, 1991). Consequently, the overall N removal efficiency became decoupled from the potential of denitrification activity. Denitrification of the $^{14}NO_3^-/^{15}NO_3^-$ mixture diffusing from the water column into the sediment responded linearly with increasing NO_3^- availability (ambient $^{14}NO_3^-$ + added $^{15}NO_3^-$, Figure 5), indicating that saturation was never reached along the ^{15}N enrichment applied in the IPT incubations. Pulse NO_3^- additions were found to stimulate denitrification rates in the ditch sediments immediately, suggesting that denitrification potential was only partially expressed in situ. These results are consistent with other studies describing a strong correlation between substrate availability and denitrification rates in sediments from drainage ditches and other agriculturally influenced waterways (Racchetti and others, 2011; Speir and others, 2017). The slope of the regression line increased sharply from spring (Figure 5a) to summer (Figure 5b), indicating that denitrification was primarily regulated by water temperature rather than by the availability of organic carbon. This was in line with previous findings in freshwater sediments, which demonstrated that higher temperatures accelerate the kinetics and efficiency of NO_3^- removal (Smith and others, 2006; Velthuis & Veraart, 2022; Gervasio and others, 2024b). No significant differences between the sediments of the two sites further confirmed that the denitrification rate was consistently controlled by NO_3^- availability across the entire range of

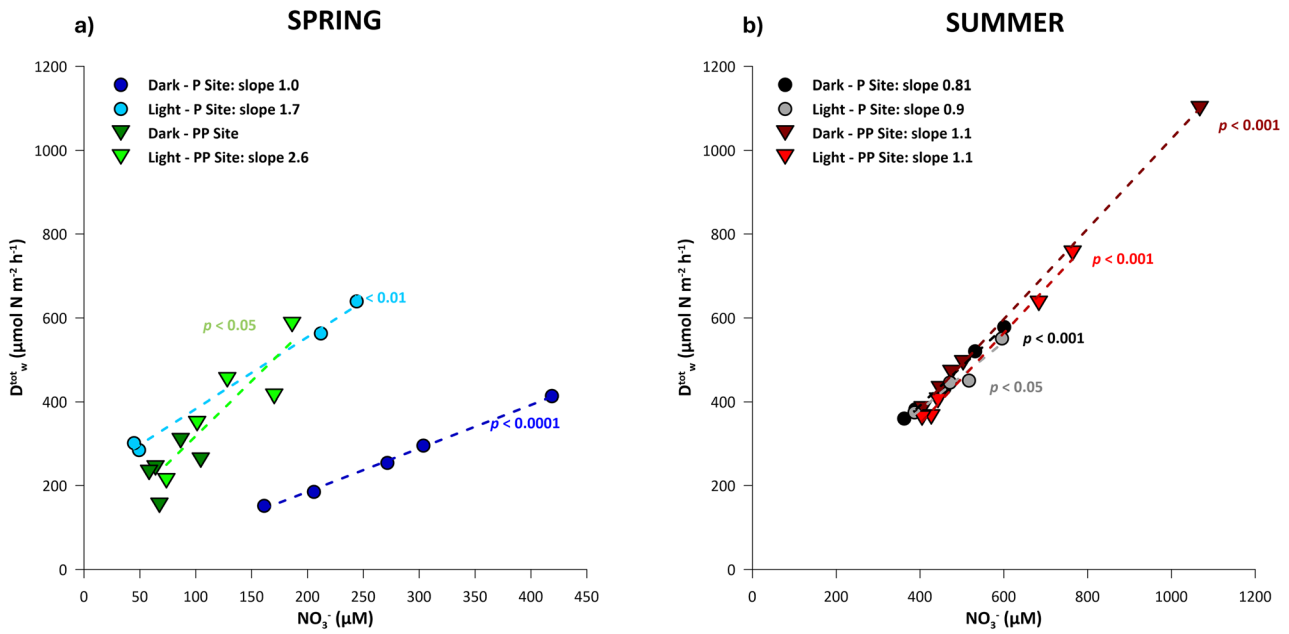


Figure 5. Denitrification of the $^{14}NO_3^-/^{15}NO_3^-$ mixture diffusing from the water column into the sediment D^{tot}_w (μmol N m^{-2} h^{-1}) correlated with the applied NO_3^- concentration (ambient $^{14}NO_3^-$ + added $^{15}NO_3^-$; μM) at both sampling sites (P and PP) in dark and light conditions during **a** spring and **b** summer sampling. The dashed lines describe the statistically significant trend.

tested concentrations. This indicated that differences in the SOM at P and PP sites did not lead to divergent denitrification responses (Wu and others, 2019; Oduor and others, 2023). SOM from LOI does not distinguish between easily degradable and more refractory pools and consequently, it is a poor proxy for the amount of labile carbon bioavailable to heterotrophic denitrifiers.

Total DNRA rates were primarily driven by the factor season ($p < 0.01$; Table 1), with higher values measured in summer, and no difference found between sites or illumination conditions. Total DNRA rates ranged between 18 ± 3 μmol N m^{-2} h^{-1} (PP site, light) and 23 ± 3 μmol N m^{-2} h^{-1} (P site, dark) in spring, and between 39 ± 11 μmol N m^{-2} h^{-1} (P site, light) and 58 ± 13 μmol N m^{-2} h^{-1} (PP site, dark) in summer (Figure 4 c, d). $DNRA_w$ dominated $DNRA_n$, accounting for an average of 88% of total rates in both seasons. The seasonal difference could be attributed to higher temperatures stimulating aerobic respiration and increasing O_2 consumption (Figure 2), as well as to the development of more reduced conditions suitable for the DNRA process (Burgin & Hamilton, 2007; Scott and others, 2008). Under low redox conditions, NO_3^- may become a limiting factor relative to the amount of available organic carbon. This promotes DNRA over denitrification, thereby recycling N within the system (Kraft and others, 2014). Overall, DNRA rates were one order of magnitude lower than corresponding denitrification rates (Figure 4), confirming that the latter was the main process responsible for NO_3^- dissipation. In spring, DNRAw accounted for ~ 6% of total NO_3^- removal. In summer, this percentage doubled to ~ 11%, which may partially explain the higher NH_4^+ effluxes from the sediments to the water column.

Contribution of Ditch Sediments to Remove Geogenic N

Denitrification has been shown to be the main process responsible for NO_3^- removal in ditch sediments, with a very low amount recycled into NH_4^+ by DNRA (6–11%) and negligible conversion to N_2O. Production of N_2O was detected at both sites in both seasons with rates ranging from 0.13 to 1.5 μmol N m^2 h^{-1} (data not shown), representing on average < 7‰ and < 2‰ in spring and summer, respectively, of the correspondent N_2 production rates by D_{tot}. These results corroborated previous in situ measurements conducted within the same canal network and revealed minimal incomplete denitrification (Castaldelli and others, 2015). In order to provide context for the N removal measurements, the denitrification capacity of the ditch sediments was compared with the N loads conveyed by the drainage ditches themselves and discharged into the main collector in spring and summer. Gaiolini and others (2026) reported flow data, which were combined with in situ NO_3^- and NH_4^+ concentrations measured during sediment sampling to calculate the average dissolved inorganic nitrogen load for each season. The estimated N loads ranged from 32 g N d^1 (60% as NO_3^- and 40% as NH_4^+) in spring to 640 g N d^{-1} (85% as NO_3^- and 15% as NH_4^+) in summer when irrigation occurred. Based on the seasonal ranges of total denitrification rates measured in the ditch sediments under study, the complete removal of N loads would require surface areas of 370–490 m^2 and 5600–6600 m^2 in spring and summer, respectively. In spring, the N load could potentially be removed by an area roughly equivalent in size to the drainage ditches under study (427 m^2), that is, to say, the system from which the load outflows. Indeed, sediment denitrification effectively counterbalances transient loads in spring. By contrast, achieving total load removal in summer would require an area approximately 14 times the size of the ditches under study. In other words, the system dissipates the entire load in spring, whereas in summer, only 6–8% of the load is removed.

In the basin under investigation, the supply of geogenic N is exacerbated in agricultural fields that are subirrigated via tile drains, as these create shortcuts between surface water and shallow groundwater bodies (Gaiolini and others, 2025). Hydrological dynamics, such as water table fluctuations, intense rainfall events and irrigation management, act as concurrent drivers in modulating the processing and transport of N loads to surface waters. Therefore, it is crucial to understand the rate at which denitrification occurs in canal networks and its impact on the N delivery to coastal zones and its availability to primary producers, particularly when the risk of eutrophication is greatest. The present study demonstrated that canal sediments exert strong control over local N loads from the unconfined aquifer, thereby contributing to their attenuation along the terrestrial–freshwater–coastal continuum. However, to ensure permanent removal before reaching the coastal zones in summer, geogenic NH_4^+ requires larger treatment areas or longer retention times. Indeed, except in spring under light conditions, ditch sediments acted as a net sink for NO_3^- and also as a source of NH_4^+ to the water column, thus potentially driving coastal eutrophication. Nitrification, a

central process in the N cycle linking the mineralization of SOM and the permanent N loss via denitrification, might be promoted by oxidized conditions sustained in the rhizosphere or in biofilms of rooted macrophytes. Aquatic vegetation can substantially enhance the N processing within ditch sediments by promoting the spatial coupling of nitrification and denitrification (Racchetti and others, 2017; Veraart and others, 2017). The oxygen released from plant roots through radial oxygen loss creates localized oxic microniches in the rhizosphere, thereby stimulating the activity of ammonia-oxidizing microorganisms and increasing the conversion of NH_4^+ to NO_3^-. The nitrate generated in the oxic zones subsequently diffuses into adjacent anoxic sediment layers, where it is reduced to N_2 via microbial denitrification (Speir and others, 2017; Soana and others, 2023). This close coupling between rhizosphere-enhanced nitrification and denitrification increases the permanent removal of reactive N from the system, improving the self-purification capacity of agricultural drainage networks.

Conclusions

Benthic metabolism in the agricultural ditches of the Po River basin was governed by a pronounced seasonal dichotomy, where the interplay between sediment lithology and environmental drivers dictated the fate of N. In spring, illuminated conditions promoted net autotrophy, with O_2 production by microphytobenthos favoring the coupled nitrification–denitrification process that effectively intercepts the geogenic N released from peaty lenses. In contrast, the transition to summer triggered a metabolic shift as high temperatures accelerate microbial respiration. Under these conditions, nitrification becomes the rate-limiting step for permanent N dissipation, due to the sedimentary O_2 consumption limiting O_2 penetration. The depletion of the oxic layer hinders the oxidation of NH_4^+ into NO_3^- and facilitates a substantial NH_4^+ efflux to the water column, partially sustained by DNRA. This indicates a critical shift from permanent N removal toward internal recycling and transport to the coastal zones, potentially triggering eutrophication.

Ultimately, peat layers act as a chronic internal source of nutrients, the impact of which is shaped by seasonal changes in biogeochemical dynamics. Eutrophic ecosystem management highlights the need to develop predictive models that consider geological heterogeneity and seasonal metabolic shifts, particularly in light of climate change scenarios projecting longer, warmer summers. Future management and restoration strategies for lowland watersheds must consider these internal geogenic sources, since they can circumvent conventional nutrient reduction measures.

Acknowledgements

The present work received financial support under the National Recovery and Resilience Plan, Mission 4, Component 2, Investment 1.1, Call for tender n° 104 published on February 2, 2022, by the Italian Ministry of University and Research, funded by the European Union–NextGenerationEU, Project NO_3EXCESS–Nitrogen Origin, EXport and Cycling in coastal irrigatEd SettingS (Grant number 2022AKA3HL). The authors would like to thank Elena Tamisari and La Sante Farm for granting access to the experimental site and for their support during the monitoring campaigns.

Funding

Open access funding provided by Università degli Studi di Ferrara within the CRUI-CARE Agreement.

Data Availability

Data used in this study are available at: https://doi.org/10.5281/zenodo.21553518.

Declarations

Conflict of interest The authors declare no conflicts of interest.

Open Access

This article is licensed under a Creative Commons Attribution 4.0 International License, which permits use, sharing, adaptation, distribution and reproduction in any medium or format, as long as you give appropriate credit to the original author(s) and the source, provide a link to the Creative Commons licence, and indicate if changes were made. The images or other third party material in this article are included in the article's Creative Commons licence, unless indicated otherwise in a credit line to the material. If material is not included in the article's Creative Commons licence and your intended use is not permitted by statutory regulation or exceeds the permitted use, you will need to obtain permission directly from the copyright holder. To view a copy of this licence, visit http://creativecommons.org/licenses/by/4.0/.

REFERENCES

Adebanjo-Aina O, Oludoye O. 2025. Impact of nitrogen fertiliser usage in agriculture on water quality. Pollutants. 5(3):21.

An S, Joye SB. 2001. Enhancement of coupled nitrification-denitrification by benthic photosynthesis in shallow estuarine sediments. Limnology and Oceanography 46(1):62–74.

APHA (American Public Health Association). 1992. Standard Methods for the Examination of Water and Wastewaters. 8th ed., Washington, DC, USA.

Armstrong FAJ, Stearns CR, Strickland JDH. 1967. The measurement of upwelling and subsequent biological process by means of the Technicon Autoanalyzer® and associated equipment. In Deep Sea Research and Oceanographic Abstracts 14(3):381–389.

Balestrini R, Delconte CA, Sacchi E, Buffagni A. 2021. Groundwater-dependent ecosystems as transfer vectors of nitrogen from the aquifer to surface waters in agricultural basins: The fontanili of the Po Plain (Italy). Science of the Total Environment 753:141995.

Basu NB, Van Meter KJ, Byrnes DK, Van Cappellen P, Brouwer R, Jacobsen BH, Jarsjö J, Rudolph DL, Cunha MC, Nelson N, Bhattacharya R, Destouni G, Olsen SB. 2022. Managing nitrogen legacies to accelerate water quality improvement. Nature Geoscience 15(2):97–105.

Bates D, Mächler M, Bolker B, Walker S. 2015. Fitting linear mixed-effects models using lme4. Journal of Statistical Software 67:1–48.

Battye W, Aneja VP, Schlesinger WH. 2017. Is nitrogen the next carbon? Earth's Future 5(9):894–904.

Bertassello LE, Basu NB, Maes J, Grizzetti B, La Notte A, Feyen L. 2025. The important role of wetland conservation and restoration in nitrogen removal across European river basins. Nature Water 3(8):867–880.

Boedecker AR, Taylor JM, Tappenbeck TH, Hall RO Jr, Robbins CJ, Scott JT. 2024. Evaluating O_2: Ar, N_2: Ar, and $^{29,30}N_2$ using membrane inlet mass spectrometry configured to minimize oxygen interference. Limnology and Oceanography: Methods 22(11):791–804.

Bower CE, Holm-Hansen T. 1980. A salicylate–hypochlorite method for determining ammonia in seawater. Canadian Journal of Fisheries and Aquatic Sciences 37(5):794–798.

Bruno L, Campo B, Hajdas I, Hong W, Amorosi A. 2022. Timing and mechanisms of sediment accumulation and pedogenesis: Insights from the Po Plain (northern Italy). Palaeogeography, Palaeoclimatology, Palaeoecology 591:110881.

Burgin AJ, Hamilton SK. 2007. Have we overemphasized the role of denitrification in aquatic ecosystems? A review of nitrate removal pathways. Frontiers in Ecology and the Environment 5(2):89–96.

Castaldelli G, Soana E, Racchetti E, Vincenzi F, Fano EA, Bartoli M. 2015. Vegetated canals mitigate nitrogen surplus in agricultural watersheds. Agriculture, Ecosystems & Environment 212:253–262.

Clifford C, Bieroza M, Clarke SJ, Pickard A, Stratigos MJ, Hill MJ, Raheem N, Tatariw C, Wood PJ, Arismendi I, Audet J, Aviles D, Bergman JN, Brown AG, Burns RE, Connolly J, Cook S, Crabot J, Cross WF, Dean JF, Evans CD, Fenton O, Friday L, Gething KJ, Giannico G, Habib W, Maher Hasselquist E, Heili NM, van der Knaap J, Kosten S, Law A, van der Lee GH, Mathers KL, Morgan JE, Rahimi H, Sayer CD, Schepers M, Shaw RF, Smiley PC Jr, Speir SL, Strock JS, Struik Q, Tank JL, Wang H, Webb JR, Webster AJ, Yan Z, Zivec P, Peacock M. 2025. Lines in the landscape. Communications Earth & Environment 6(1):693.

Colombani N, Mastrocicco M, Castaldelli G, Aravena R. 2019. Contrasting biogeochemical processes revealed by stable isotopes of H_2O, N, C and S in shallow aquifers underlying agricultural lowlands. Science of the Total Environment 691:1282–1296.

Dalsgaard T, Nielsen LP, Brotas V, Viaroli P, Underwood G, Nedwell D, Sundbäck K, Rysgaard S, Miles A, Bartoli M, Dong L, Thornton DCO, Ottosen LDM, Castaldelli G, Risgaard Petersen N. 2000. Protocol handbook for NICE-Nitrogen Cycling in Estuaries: a project under the EU research programme: Marine Science and Technology (MAST III). Ministry of Environment and Energy National Environmental Research Institute. Denmark: Department of Lake and Estuarine Ecology. p1–62.

de Klein JJ, Overbeek CC, Juncher Jørgensen C, Veraart AJ. 2017. Effect of temperature on oxygen profiles and denitrification rates in freshwater sediments. Wetlands 37(5):975–983.

de la Paz M, Ferrón S, Borges A, Upstill-Goddard RC. 2021. Standard Operating Protocol: Quantification of methane and nitrous oxide via headspace equilibrium. https://hdl.handle.net/2268/253977

de Vries, W., Posch, M., Simpson, D., de Leeuw, F. A., van Grinsven, H. J., Schulte-Uebbing, L. F., ... & Ros, G. H. 2024. Trends and geographic variation in adverse impacts of nitrogen use in Europe on human health, climate, and ecosystems: A review. Earth-Science Reviews 253:104789.

Fox J, Weisberg S. 2019. An R companion to applied regression. Sage publications. https://www.john-fox.ca/Companion/

Gaiolini M, Colombani N, Chierici V, Montanari L, Mastrocicco M. 2025. Numerical modelling of groundwater level and salinity evolution in a low-lying coastal area under intensive agricultural activity. Water Resources Management 39(4):1747–1761.

Gaiolini M, Sbarbati C, Ofori A, Macumu PH, Gervasio MP, Tamisari E, Vincenzi F, Soana E, Castaldelli G, Piscopo V, Mastrocicco M, Colombani N. 2026. Salt migration and export via subsurface irrigation in a saline reclaimed landscape of the Po River lowland (Italy). Journal of Hydrology 134563.

Gervasio MP, Castaldelli G, Soana E. 2024b. The response of denitrification to increasing water temperature and nitrate availability: the case of a large lowland river (Po River, Northern Italy) under a Climate Change Scenario. Environments 11(8):179.

Gervasio MP, Soana E, Gavioli A, Vincenzi F, Castaldelli G. 2024a. Contrasting effects of climate change on denitrification and nitrogen load reduction in the Po River (Northern Italy). Environmental Science and Pollution Research 31(35):48189–48204.

Gervasio MP, Soana E, Vincenzi F, Castaldelli G. 2022. An underestimated contribution of deltaic denitrification in reducing nitrate export to the coastal zone (Po River-Adriatic Sea, Northern Italy). Water 14(3):501.

Kana TM, Darkangelo C, Hunt MD, Oldham JB, Bennett GE, Cornwell JC. 1994. Membrane inlet mass spectrometer for rapid high-precision determination of N_2, O_2, and Ar in environmental water samples. Analytical Chemistry 66(23):4166–4170.

Kraft B, Tegetmeyer HE, Sharma R, Klotz MG, Ferdelman TG, Hettich RL, Geelhoed JS, Strous M. 2014. The environmental

controls that govern the end product of bacterial nitrate respiration. Science 345(6197):676–679.

Lewandowski J, Meinikmann K, Krause S. 2020. Groundwater–surface water interactions: Recent advances and interdisciplinary challenges. Water 12(1):296.

Liu W, Du Y, Ning J, Zheng S, Qiu W, Wang Y. 2026. Geogenic ammonium enrichment in alluvial-lacustrine aquifer systems: coupled controls of microbial pathways and organic matter composition. Environmental Science & Technology 60(2):2088–2100.

Lorenzen CJ. 1967. Determination of chlorophyll and pheopigments: spectrophotometric equations 1. Limnology and Oceanography 12(2):343–346.

Macumu PH, Gaiolini M, Ofori A, Mastrocicco M, Colombani N. 2024. Additional sources of salinity and heavy metals from plant residues of peaty horizons in the Po River lowland (Italy). Science of the Total Environment 957:177671.

Mastrocicco M, Giambastiani BMS, Colombani N. 2013. Ammonium occurrence in a salinized lowland coastal aquifer (Ferrara, Italy). Hydrological Processes 27(24):3495–3501.

Nielsen LP. 1992. Denitrification in sediment determined from nitrogen isotope pairing. FEMS Microbiology Letters 86(4):357–362.

Nikolaidis NP, Phillips G, Poikane S, Várbíró G, Bouraoui F, Malagó A, Lilli MA. 2022. River and lake nutrient targets that support ecological status: European scale gap analysis and strategies for the implementation of the Water Framework Directive. Science of the Total Environment 813:151898.

Oduor BO, Campo-Bescós MÁ, Lana-Renault N, Casalí J. 2023. Effects of climate change on streamflow and nitrate pollution in an agricultural Mediterranean watershed in Northern Spain. Agricultural Water Management 285:108378.

Owens MS, Cornwell JC. 2016. The benthic exchange of O_2, N_2 and dissolved nutrients using small core incubations. Journal of Visualized Experiments 114:e54098.

Pina-Ochoa E, Álvarez-Cobelas M. 2006. Denitrification in aquatic environments: a cross-system analysis. Biogeochemistry 81(1):111–130.

Racchetti E, Bartoli M, Soana E, Longhi D, Christian RR, Pinardi M, Viaroli P. 2011. Influence of hydrological connectivity of riverine wetlands on nitrogen removal via denitrification. Biogeochemistry 103(1):335–354.

Racchetti E, Longhi D, Ribaudo C, Soana E, Bartoli M. 2017. Nitrogen uptake and coupled nitrification–denitrification in riverine sediments with benthic microalgae and rooted macrophytes. Aquatic Sciences 79(3):487–505.

Richardson K, Steffen W, Lucht W, Bendtsen J, Cornell SE, Donges JF, Drüke M, Fetzer I, Bala G, von Bloh W, Feulner G, Fiedler S, Gerten D, Gleeson T, Hofmann M, Huiskamp W, Kummu M, Mohan X, Nogués-Bravo D, Petro S, Porkka M, Rhmstorf S, Schaphoff S, Thonicke K, Tobian A, Virkki V, Wang-Erlandsson L, Weber L, Rockström J. 2023. Earth beyond six of nine planetary boundaries. Science advances 9(37): eadh2458.

Risgaard-Petersen N, Nielsen LP, Rysgaard S, Dalsgaard T, Meyer RL. 2003. Application of the isotope pairing technique in sediments where anammox and denitrification coexist. Limnology and Oceanography: Methods 1(1):63–73.

Risgaard-Petersen N, Rysgaard S. 1995. Nitrate reduction in sediments and waterlogged soil measured by 15N techniques. In Methods in Applied Soil Microbiology and Biochemistry, Academic Press. p287–295.

Robertson EK, Bartoli M, Brüchert V, Dalsgaard T, Hall PO, Hellemann D, Hietanen S, Zilius M, Conley DJ. 2019. Application of the isotope pairing technique in sediments: use, challenges, and new directions. Limnology and Oceanography: Methods 17(2), 112–136.

Romero E, Garnier J, Lassaletta L, Billen G, Le Gendre R, Riou P, Cugier P. 2013. Large-scale patterns of river inputs in southwestern Europe: seasonal and interannual variations and potential eutrophication effects at the coastal zone. Biogeochemistry 113(1):481–505.

Romero E, Ludwig W, Sadaoui M, Lassaletta L, Bouwman AF, Beusen AH, van Apeldoorn D, Sardans J, Janssens IA, Ciais P, Obersteiner M, Peñuelas J. 2021. The Mediterranean region as a paradigm of the global decoupling of N and P between soils and freshwaters. Global Biogeochemical Cycles 35(3): e2020GB006874.

Rysgaard S, Risgaard-Petersen N, Niels Peter S, Kim J, Lars Peter N. 1994. Oxygen regulation of nitrification and denitrification in sediments. Limnology and Oceanography 39(7):1643–1652.

Sawyer AH, Michael HA, Schroth AW. 2016. From soil to sea: the role of groundwater in coastal critical zone processes. Wiley Interdisciplinary Reviews: Water 3(5):706–726.

Schlesinger WH. 2009. On the fate of anthropogenic nitrogen. Proceedings of the National Academy of Sciences 106(1):203–208.

Scott JT, McCarthy MJ, Gardner WS, Doyle RD. 2008. Denitrification, dissimilatory nitrate reduction to ammonium, and nitrogen fixation along a nitrate concentration gradient in a created freshwater wetland. Biogeochemistry 87(1):99–111.

Shen W, Li S, Mi M, Zhuang Y, Zhang L. 2021. What makes ditches and ponds more efficient in nitrogen control? Agriculture. Ecosystems & Environment 314:107409.

Smith LK, Voytek MA, Böhlke JK, Harvey JW. 2006. Denitrification in nitrate-rich streams: Application of N_2: Ar and ^{15}N-tracer methods in intact cores. Ecological Applications 16(6):2191–2207.

Soana E, Gavioli A, Neri F, Castaldelli G. 2023. Looking back to move forward: Restoring vegetated canals to meet missing Water Framework Directive goals in agricultural basins. Science of the Total Environment 905:167331.

Speir SL, Tank JL, Taylor JM, Grose AL. 2023. Temperature and carbon availability interact to enhance nitrous oxide production via denitrification in alluvial plain river sediments. Biogeochemistry 165(2):191–203.

Speir SL, Taylor JM, Scott JT. 2017. Seasonal differences in relationships between nitrate concentration and denitrification rates in ditch sediments vegetated with rice cutgrass. Journal of Environmental Quality 46(6):1500–1509.

Steingruber SM, Friedrich J, Gächter R, Wehrli B. 2001. Measurement of denitrification in sediments with the 15N isotope pairing technique. Applied and Environmental Microbiology 67(9):3771–3778.

Sundbäck K, Enoksson V, Granéli W, Pettersson, K. 1991. Influence of sublittoral microphytobenthos on the oxygen and nutrient flux between sediment and water: a laboratory continuous-flow study. Marine Ecology Progress Series 263–279.

Velthuis, M., & Veraart, A. J. 2022. Temperature sensitivity of freshwater denitrification and N_2O emission-A meta-analysis. Global Biogeochemical Cycles 36(6): e2022GB007339.

Veraart AJ, Dimitrov MR, Schrier-Uijl AP, Smidt H, de Klein JJ. 2017. Abundance, activity and community structure of denitrifiers in drainage ditches in relation to sediment characteristics, vegetation and land-use. Ecosystems 20(5):928–943.

Warembourg FR. 1993. Nitrogen fixation in soil and plant systems. In Nitrogen isotope techniques 654: 157–80. Knowles, R. & Blackburn, T.H. eds.

Weiss RF. 1970. The solubility of nitrogen, oxygen and argon in water and seawater. Deep sea research and oceanographic abstracts Elsevier, p. 721–735.

Weiss RF, Price BA. 1980. Nitrous oxide solubility in water and seawater. Marine Chemistry 8(4):347–359.

Wu S, Wu Z, Liang Z, Liu Y, Wang Y. 2019. Denitrification and the controlling factors in Yunnan Plateau Lakes (China): exploring the role of enhanced internal nitrogen cycling by algal blooms. Journal of Environmental Sciences 76:349–358.

Xiong Y, Du Y, Zhang J, Zhao X, Li Q, Deng Y, Wang Y. 2025. Salinity-Organic Matter Coupling Facilitates Geogenic Ammonium Enrichment in Coastal Aquifer Systems. Environmental Science & Technology 59(30):15828–15842.

Zilius M, Daunys D, Petkuviene J, Bartoli M. 2012. Sediment-water oxygen, ammonium and soluble reactive phosphorus fluxes in a turbid freshwater estuary (Curonian lagoon, Lithuania): evidences of benthic microalgal activity. Journal of Limnology 71(2):309–319.